Experimental optimization of Microbially Induced Calcite Precipitation (MICP) for contact erosion control in earth dams

A. Clarà Saracho & S. K. Haigh
University of Cambridge, Cambridge, United Kingdom

ABSTRACT: Microbial induced calcite precipitation (MICP) is a bio-mediated soil improvement technique which is low-cost, low-maintenance and non-disruptive to wild life and aesthetics. It holds the potential for simultaneously retaining the hydraulic conductivity, increasing the shear resistance and preferentially cementing the interface between coarse and fine particles. Previous studies have shown that, unlike other biocementation works – such as liquefaction control and railroad embankment stabilisation – the shear strength increase necessary on interfaces vulnerable to contact erosion in earth dams is very low, requiring different optimal MICP treatment formulations to be explored. The study presented herein focuses on MICP treatment across the boundary between a fine sand and a coarse sand in the context of one-dimensional flow column experiments. Treatment optimisation is evaluated by varying important parameters including formulations of chemical amendments, and the particle size distribution of the fine grained fraction. Subsequently, a procedure is developed for measuring the calcite bond shear strength using an Erosion Function Apparatus (EFA), whereby an undisturbed MICP treated specimen is slowly protruded into a flume and eroded by surface-parallel flow. Measurements of the surface movement of the eroding sample are made with a laser reflecting on the soil surface in the flume. The progress of erosion can hence be monitored as the flow velocity is increased. Results open up new interesting perspectives on the treatment scheme needed for MICP implementation for contact erosion control in dams.

1 INTRODUCTION

Internal erosion is responsible for almost 50% of all embankment dam failures (ICOLD 2016). Although embankment dam engineering has increasingly evolved over the last century, it remains very difficult to assess the long-term performance of existing dams, because they may have significant deficiencies in regards to material capability. This is the case of the downstream granular filters of many older structures, which, if at all existent, may not necessarily reflect current filter design practice, making them susceptible to contact erosion (CE). This phenomenon develops at the interface between two soils with different grain sizes and permeabilities due to the shear stress of interface-parallel flow and can thus occur at the downstream edge of the core-filter interface and along the core-foundation boundary (Figure 1). Although the hydraulic gradient in both layers is approximately the same, the difference in permeability will cause the velocity in the coarse layer to be much higher than that in the fine one. This velocity gradient will induce a shear stress on the upper particles of the fine layer, triggering detachment. If these particles find an unfiltered exit, erosion will initiate.

ICOLD (2016) distinguishes two different approaches to control internal erosion: filters and barriers. While they are both sensible methods to reduce the risk of internal erosion, in the long term, filter effectiveness within the dam may be reduced and new pathways may open up around these barriers. In addition, although established cement-based methods are able to reduce internal erosion effectively, they often end up shifting the seepage flow from grouted channels to previously dry ones, increasing pore pressures and, with them, the risk of failure in the structure. This makes current solutions insufficient and force the consideration of new biochemical techniques.

Within this context, microbial induced calcite precipitation (MICP), a bio-mediated soil improvement technique that leads to the binding of soil grains by carbonate crystals, is a viable alternative. Previous studies have shown that this process holds the potential for simultaneously retaining the hydraulic conductivity of the soil, improving its erodibility, and

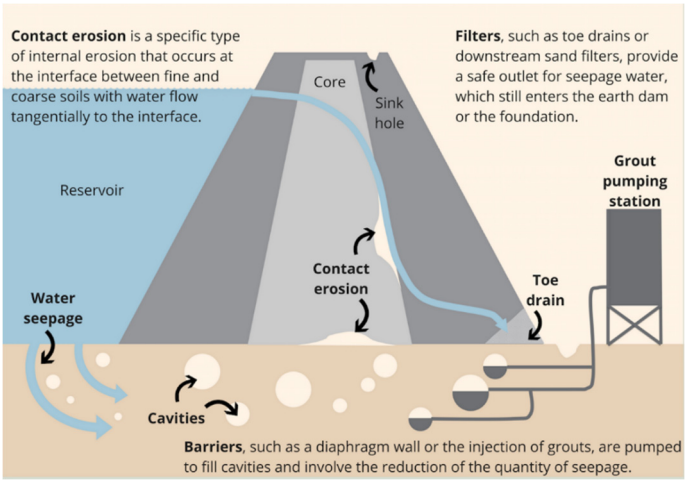

Figure 1. Schematic diagram of the possible locations of contact erosion and existing control measures.

preferentially cementing the interface between coarse and fine particles (Clarà Saracho & Haigh 2018). These three attributes make it particularly attractive for CE control.

Yet, little is known about erosion of MICP treated sands, despite being ranked as the first most feasible application for biogeochemical soil improvement techniques, together with structural repair, dust mitigation, and immobilisation of contaminants (Dejong et al. 2013). To date, Jiang (2016) has been the only one to study its potential for the mitigation of internal suffusion in earth dams, and found an increase in both the critical hydraulic gradient and the shear resistance. Nonetheless, its behaviour in the presence of an interface subject to the parallel shear force imposed by water remains unexplored. For this reason, an Erosion Function Apparatus (EFA), shown in Figure 2, was developed to quantify the erosion of undisturbed MICP treated sands.

MICP by urea hydrolysis is the most widely used biomediated soil improvement technique to date (DeJong et al. 2010). This process occurs through the hydrolysis reaction of urea as a bacteria metabolism process, which primes the availability of carbonate ions, producing calcium carbonate (calcite) in the presence of calcium (Stocks-Fischer et al. 1999). The current study uses the bacterium *Sporosarcina pasteurii* to harbour urea hydrolysis, which happens in conjunction with the generation of ATP, a form of intracellular energy transfer (Jahns 1996; Whiffin 2004; Mujah et al. 2016). Unlike many other microorganisms, this enables *S. pasteurii* to produce urea in the presence of ammonium, a vital characteristic for the hydrolysis reaction itself (Whiffin 2004).

The study presented herein experimentally evaluates different MICP chemical amendments and particle size distributions in the context of one-dimensional flow column experiments. It focuses on providing insights into the effects of MICP treatment on erosion patterns and the total amount eroded for erosion control in water retaining structures. Indeed, while liquefaction control or railroad embankment stabilisation may require calcite concentrations of as high as 30% (Van Paassen et al. 2010), this value is substantially reduced for earth dams (Clarà Saracho & Haigh 2018). Therefore, very low urea and calcium concentrations were tested.

2 EXPERIMENTAL PROC EDURES

2.1 *Materials and methods*

2.1.1 *Specimen setup and preparation*

Acrylic PTFE cylindrical cores (32.12 × 100 mm) were dry packed with a filter-soil layer consisting of 35 mm of Fraction A silica sand (D_{50} = 1.61 mm) overlying a base-soil layer consisting of 25 mm of Fraction D (D_{50} = 0.165 mm, e_{min} = 0.585, e_{max} = 0.988) or Fraction E (D_{50} = 0.140 mm, e_{min} = 0.613, e_{max} =1.014) silica sand.

The cores were oriented vertically with acrylic top and bottom caps, and a metallic filter mesh was placed adjacent to the bottom cap to prevent soil migration out of the cores. Additionally, bottom ports were fitted with tubbing to allow drainage and full control of saturation conditions during MICP treatment.

2.1.2 *Applied treatment procedure*

Each specimen was saturated before treatment to remove air pockets, ensure a controlled flow field, and determine the pore volume (PV).

Subsequently, a two-phase injection scheme was used. In the first (biological phase), 1 PV of the bacteria solution was injected from the top by gravity and left to set within the specimen for a retention period (24 hours) to allow for microbes to attach to the particles (DeJong et al. 2006). In the second (cementation) phase, 1 PV of the nutrient solution was injected in the same way and the old solution was allowed to drain out of the specimen. For the cementation phase, different formulations were tested. These are referred to in Table 1 with recipe labels describing the molar concentrations.

Table 1. Cementation treatment formulations.

Chemical name	Chemical formula	Recipe		
		A	B	C
Urea	$CO(NH_2)_2$	0.06 M	0.09 M	0.375 M
Calcium chloride	$CaCl_2$	0.04M	0.06 M	0.25 M
Sodium bicarbonate	$NaHCO_3$	2.12 g/L	2.12 g/L	2.12 g/L
Nutrient broth		3 g/L	3 g/L	3 g/L

Treatment was terminated after 10 injections of the cementation solution. The liquid medium was first drained and the soil flushed with deionised water to remove excess material.

2.1.3 *Treatment monitoring*

Calcium carbonate content was determined after treatment completion by using inductively coupled plasma optical emission spectrometry (ICP-OES). By dissolving samples obtained from the MICP treated specimens in 1M hydrochloric acid, a solution containing calcium ions is obtained. The ICP-OES machine then excites the calcium ions, which consequently emit electromagnetic radiations at their individual characteristic wavelengths. Hence, this technique enables the identify and quantity of the elements present in the solution.

2.2 *Flume design*

An Erosion Function Apparatus (EFA), shown in Figure 2, was designed to measure the erosion of specimens at varying shear stresses. Similar setups have previously been described by McNeil et al. (1996), Roberts (1998), Ravens & Gschwend (1999), and Briaud et al. (2001). The EFA is essentially a 1 m long straight flume with a width and height of 60 mm and 25 mm, respectively. The main components are the coring tube; the test section; an inlet section with a flow straightener to stimulate development of the bottom boundary layer; a flow exit section; a water storage tank; and a pump (Pedrollo PQAm 90). In addition, a water delivery system (Figure 3) is used to monitor the water flow rate and pressure delivered to the flume. This consists of a control valve, which provides control over the flow rate in the flume, and a flow meter (RS 253-133), positioned between the pump and the valve.

At the start of each test, a 1D actuator (RS 764-3477) was used to drive the specimen through the circular opening in the bottom of the test section until it protruded 1 mm from the bottom of the flume. Water was pumped through the flume, imposing a shear stress on the specimen, and causing it to erode. A laser (Baumer 12I6460/S35A) reflecting on the centre of soil surface in the flume was configured to continually activate the actuator so that the soil-water interface remained at 1 mm above the bottom of the flume. The progress of erosion was recorded as the upward movement of the specimen in the coring tube by means of an LVDT (Schlumberger M811750-67).

The Data Acquisition Toolbox was used to configure the data acquisition hardware and read data into Matlab for immediate analysis. The toolbox interface uses analog input and output objects, each represented by multiple channels, to communicate with a Measurement Computing™ device. A session was configured to acquire data at 100 Hz, based on the duration of each flow rate step (30 minutes).

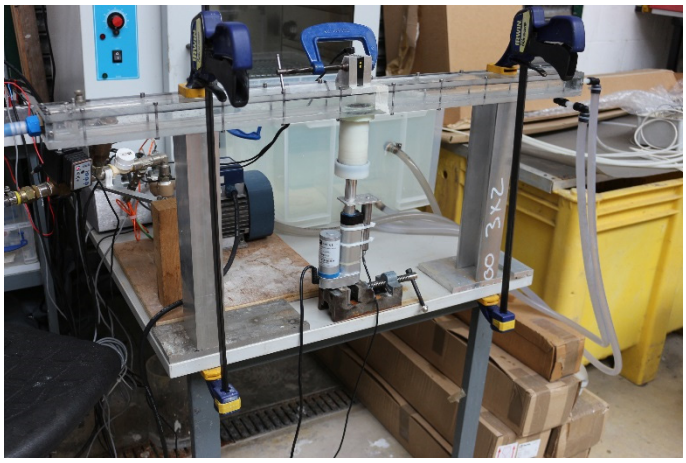

Figure 2. EFA experimental setup.

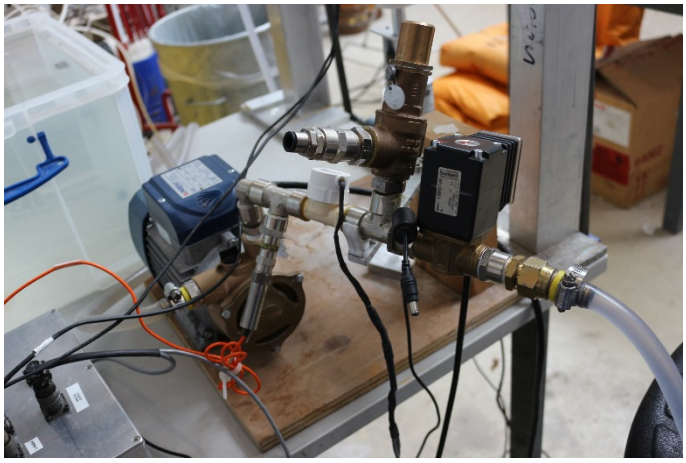

Figure 3. Water delivery system.

2.2.1 *Hydrodynamics*

An important principle behind the flume operation was the relationship between the flow rate Q (l/min) through the flume and the shear stress τ (Pa) applied to the specimen. This connection was made using the Darcy-Weisbach equation, relating τ with the cross-section averaged velocity U (m s^{-1}) by means of a friction factor f:

$$\tau = \frac{1}{8}\rho f U^2 \quad (1)$$

where ρ = water density (kg m^{-3}). The Moody chart (Moody 1944), modified for flow through a rectangular pipe, provided the friction factor as a function of the flow regime, characterized by the Reynolds number, and the relative roughness.

2.2.2 *Measurement of cumulative height eroded*

The procedure for measuring the cumulative erosion of specimens as a function of shear stress and specimen height was as follows. The specimens were prepared as described above and moved upward into the test section until the sediment surface protruded 1 mm into the flume. PTFE tubes were used as soil columns because they are non-reactive and interfere with the ability of bacteria to adhere to its surface, allowing the extraction of the specimens without damaging

them. This enabled specimens with a low calcite concentration to be tested without being disturbed.

In order to measure erosion at different flow rates using only one specimen, every test started at 1.7 l/min. The flume was run sequentially at higher flow rates, with each succeeding step lasting for 30 minutes and being approximately 1.5 l/min higher than the previous one. This produced bottom shear stresses ranging from 0.0043 N/m^2 to 0.17 N/m^2, corresponding to 1.7 L/min and 16.6 L/min, respectively. Every cycle was repeated until all of the fine fraction was eroded.

3 RESULTS AND DISCUSSION

Calcite content

In order to investigate the effect of the interface on the spatial uniformity of cementation, the calcite content of five different specimens was measured. For this, cementation amendments following Recipe C (Table 1) were administered in the same fashion as previously described, except that for each one the total number of pore volumes injected was different.

As expected, calcite content increased with the number of injections. Interestingly, however, results consistently showed a preferential cementation near the interface, approximately 2-times greater than in the bulk material (Figure 4). This could be attributed to the spatially varying attached bacteria distributions along the specimen. Ford & Harvey (2007) recognised the role of chemotaxis for the migration of bacteria towards "increasing concentrations of chemicals that they perceive as beneficial to their survival." During the first injections, the cementation medium is accumulated at the interface due to the hydraulic constraint imposed by the fine sand (the velocity of the solution is significantly reduced when flowing from a high to a low permeability material). Since bacteria are able to sense through receptor molecules, they respond to this chemical gradient and preferentially attach to the soil grains located at the interface (Ford & Harvey 2007).

In addition, the calcium carbonate precipitation efficiency was calculated as the ratio of the total amount of calcium carbonate precipitated to the total amount of calcium injected as follows:

$$CaCl_2 + H_2O \rightarrow Ca^{2+} + 2Cl^- \quad (2)$$

$$CO_3^{2-} + Ca^{2+} \rightarrow CaCO_3 \quad (3)$$

$$\text{Efficiency (\%)} = \frac{[CaCO_3(s)]_T \cdot {}^{1\text{ mol } Ca^{2+}}/_{1\text{ mol } CaCO_3(s)}}{[CaCl_2]_T \cdot {}^{1\text{ mol } Ca^{2+}}/_{1\text{ mol } CaCl_2}} \quad (4)$$

where $[CaCO_3(s)]_T$ is the total amount of calcium carbonate measured after treatment, and $[CaCl_2]$ is the total amount of calcium chloride injected into the specimen during treatment. As shown in Figure 5, precipitation efficiency was higher for the specimens with the lowest calcium carbonate content. Experiments conducted by Rebata-Landa (2007) and Van Paassen (2009) also reported this stagnation in precipitation, starting after the injection of 6 to 8 pore volumes of the cementation solution, and it was associated with a bacterial activity drop. After precipitation the pore space is reduced, resulting in bacteria being trapped inside the pores and preventing the cementation solution from reaching them. This phenomenon is known as bacteria encapsulation and starvation (Van Paassen 2009). This hydraulic constraint partially interrupts the precipitation in the fine fraction and causes the cementation solution to remain in the coarse one, favouring higher chemical efficiencies near the interface. Hence, a low number of injections effectively optimises MICP.

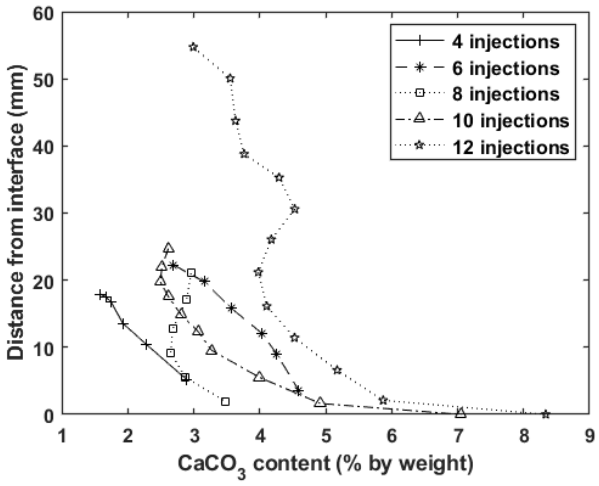

Figure 4. Effect of the interface and the number of injections of the cementation solution on the calcite content (Fraction D sand).

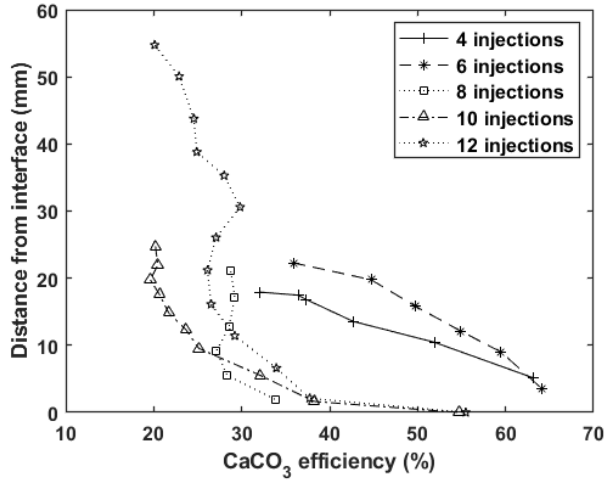

Figure 5. Effect of the interface and the number of injections of the cementation solution on the calcite precipitation efficiency (Fraction D sand, Recipe C).

3.1 *Erosion patterns as a function of calcite content*

By the procedures described, cumulative height eroded of non-MICP and MICP treated specimens were determined as a function of height and bottom shear stress. Results indicated a change of erosion process and a significantly reduced sediment erodibility.

The erosion time series were analysed by examining the cumulative height eroded as a function of time (Figure 6). For the baseline test (unreinforced specimen), results showed a sustained movement of particles. It is worth pointing out, however, that for shear stresses under 0.15 N/m^2 (16 L/min) no more than 0.5 mm of sediments eroded after evert 30-minute step. In addition, each flow rate step was accompanied by a short-lived erosion increase, the size of which was generally less than 50 µm, followed by a plateau or relaxation. This was attributed to the surface washing of the smallest and easy-to-move particles leaving a pit or hole. Conversely, higher flow intensities (producing shear stresses over 0.15 N/m^2) resulted in a more sustained movement of particles with an asymptotic tendency to permanent erosion (Philippe et al. 2013). As more soil particles participated in the process of erosion, transport, and deposition, individual steps became less apparent and a constant erosion rate of approximately 2 mm/h was established. Thus, there seemed to be a threshold between transient and persistent erosion.

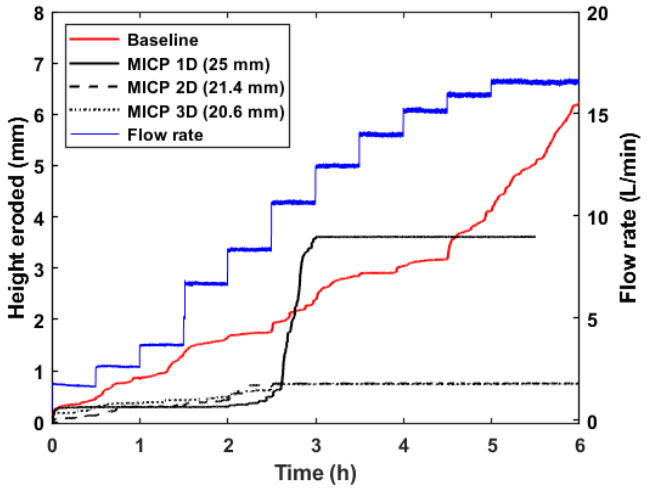

(a)

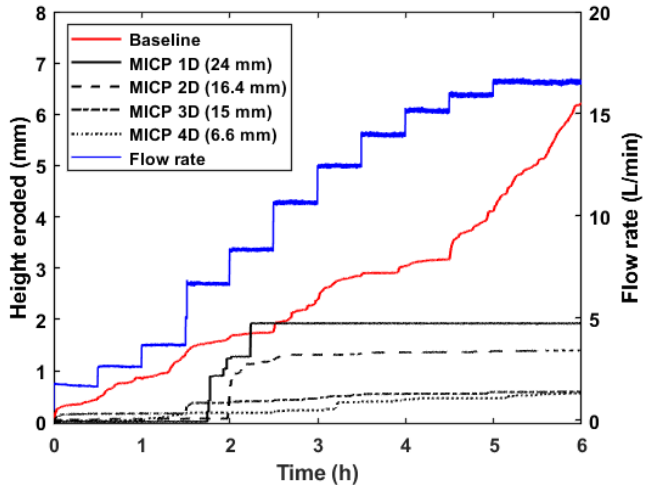

(b)

Figure 6. Erosion curves for Fraction D silica: (a) Recipe A; (b) Recipe B.

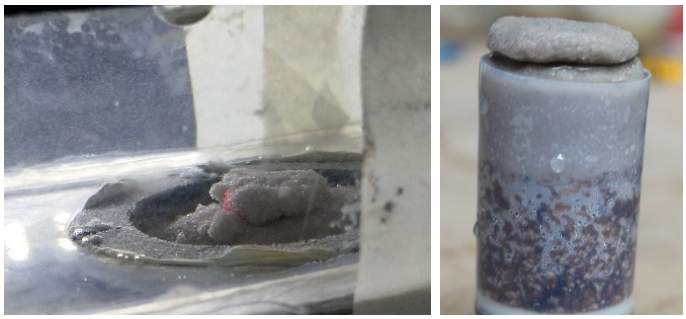

(a) (b)

Figure 7. Height-dependence of block size (Recipe B): (a) during MICP 1D test (24 mm); (b) after test MICP 2D (15mm).

The behaviour of MICP treated specimens mainly differed in three aspects. First, the relaxation of the erosion through time was total, with erosion finally ceasing for the higher flow rates. This was thought to be due to the selective erosion of the weakly cemented particles first, which progressively reinforced the mechanical resistance at the surface until only the stronger calcite-to-calcite bonds were left.

Second, the erosion process was thought to be a combination of particulate and bulk erosion. For low flow rates producing bottom shear stresses ranging between 0.004 and 0.08 N/m^2, specimens were eroded primarily in particulate form. At higher shear stresses, however, bulk erosion became predominant, as blocks of up to 10 mm in thickness were loosened. As shown in Figure 7, the size of these chunks or blocks increased with the calcium carbonate content, and hence as the distance from the interface decreased. If the shear stress imposed by the water became large enough, they were plucked from the surface and transported downstream. When this happened, a new group of weaker interparticle bonds was exposed and, occasionally, an initial surface washing was observed again.

Third, experiments also showed an increase in the critical shear stress. At low shear stresses, less than 0.03 N/m^2, very small amounts of sediment (Recipe A) or almost no sediments moved (Recipe B). This behaviour clearly juxtaposed with the one observed for untreated specimens, where erosion was observed from the start.

Sediment erodibility was also affected by the distance from the interface (value shown in parenthesis) and the cementation amendment formulation. As shown in Figure 6, erosion reductions between tests MICP 1D and MICP 2D were over twice when using Recipe A. This agrees with the chemical efficiencies and precipitation patterns described before: lower calcite contents yield less uniform efficiencies; hence,

the difference in the amount eroded is expected to be greater over smaller height differences.

3.2 *Correlation between erosion and particle size distribution*

A first attempt to establish the impact of pore and grain size on MICP treatment and erosion patterns was also carried out. For this purpose, Fraction E silica sand (D_{50} = 0.140 mm) was used. The impact was already apparent in these exploratory tests and, by comparison with the Fraction D sand, for the same treatment formulation (Recipe B) and number of injections (10 injections), the degree of cementation decreased. In addition, Figure 8 shows that unreinforced Fraction E sand (baseline) had a dramatically higher erosion rate, of almost 16 mm/h, and that there was an effective disappearance of the relaxation of erosion through time.

When reinforced with MICP, the sediments were still observed to erode primarily in particulate form, but there was an increase in the critical shear stress (to approximately 0.01 N/m^2). Unlike for the Fraction D specimens, where very strong calcite blocks were left at the vicinity of the interface, erosion of the whole specimen occurred rapidly (in only one test) and only small clusters were observed near the interface (Figure 9).

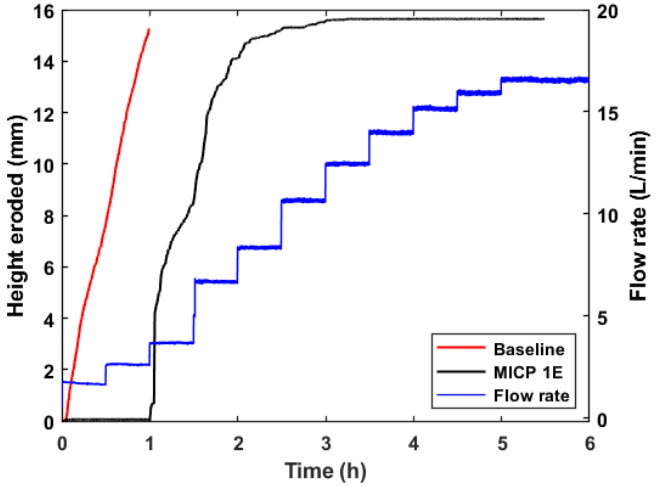

Figure 8. Erosion curves for Fraction E silica sand (Recipe B).

(a) (b)

Figure 9. MICP-treated Fraction E silica sand (a) during and (b) after MICP 1E test (Recipe B).

4 CONCLUSIONS

Implementation of laboratory-tested techniques in the field depends on understanding how the modification of soil characteristics due to MICP treatment may provide additional opportunities over other existing technologies and, more importantly, on identifying the level of improvement required for a particular application. Previous studies have already demonstrated that high chemical concentrations are not required for contact erosion control in water retaining structures (such as dams, levees, and dykes); hence, this paper focused on very low cementation treatment amendments. Undisturbed sand specimens were tested in an Erosion Function Apparatus (EFA), where they were subjected to a shear force parallel to the eroding surface. The following conclusions were obtained:

a) Bacteria were found to exhibit chemotactic responses, yielding calcite concentrations approximately 2-times greater near the interface. However, while chemical efficiencies in weakly cemented specimens were found to linearly increase with the distance from the interface, strongly cemented ones showed a stagnation in precipitation. This is something to bear in mind both for future experiments and field applications, as many injections could potentially result in a waste of reactants.
b) MICP treatment modified the erosion resistance properties of fine sands. Aside from attaining a significant reduction in the cumulative height eroded, being this of over 70% for the MICP-treated Fraction D sands, erosion patterns were significantly different. While unreinforced specimens were observed to erode primarily in particulate form, MICP-treated samples predominantly eroded block by block. The size of these blocks increased with the calcium carbonate content. In addition, it is thought that the formation of these clusters was fundamentally responsible for the erosion relaxation, this being either partial or total.
c) In comparison with the Fraction D sand, the untreated Fraction E sand not only eroded remarkably fast, but also without any local relaxation through time. In contrast, when MICP-treated, the amount eroded was reduced and the critical shear stress increased. It is worth pointing out, however, that overall calcium carbonate concentrations were lower and longer treatments may be required for fine sands.
d) From a practical standpoint, MICP treatment increased the critical shear stresses to around 0.05 N/m^2 and 0.01 N/m^2, for the Fraction D and E sands, respectively. Typical values encountered in real dams range from 0.002

N/m^2, for clays and silts, to 0.172 N/m^2, for well-graded sands. Hence, the use of low cementation treatment amendments clearly holds strong potential for erosion control in water retaining structures.

More studies are presently being done to further examine the erosional characteristics of MICP treated sands as a function of height and grain size. Erosion time series will be analysed both by examining the erosion rates in relation to the bottom shear stress and the cumulative height eroded as a function of the time-integrated shear stress, similar to Ravens & Gschwend (1999). The overarching aim will be to establish an erosional model for MICP-treated fine sands.

5 ACKNOWLEDGEMENTS

The authors would like to thank Mr Chris Knight for the production of the EFA device and EPSRC for funding this studentship as part of the Centre for Doctoral Training in Future Infrastructure and Built Environment (EP/L016095/1).

6 REFERENCES

Briaud et al., 2001. Erosion Function Apparatus for Scour Rate Predictions. *Journal of Geotechnical and Geoenvironmental Engineering*, 127(2), pp.105–113. Available at: http://ascelibrary.org/doi/10.1061/%28ASCE%291090-0241%282001%29127%3A2%28105%29.

Clarà Saracho, A. & Haigh, S., 2018. Microbially Induced Calcite Precipitation (MICP) to mitigate contact erosion in earth dams and levees. In *38th USSD Annual Conference and Exhibition*.

Dejong, J.T. et al., 2013. Biogeochemical processes and geotechnical applications: progress, opportunities and challenges. *Géotechnique*, 63(4), pp.287–301. Available at: http://www.icevirtuallibrary.com/doi/10.1680/geot.SIP13.P.017.

DeJong, J.T. et al., 2010. Bio-mediated soil improvement. *Ecological Engineering*, 36(2), pp.197–210. Available at: http://linkinghub.elsevier.com/retrieve/pii/S0925857409000238.

DeJong, J.T., Fritzges, M.B. & Nüsslein, K., 2006. Microbially induced cementation to control sand response to undrained shear. *Journal of Geotechnical and Geoenvironmental Engineering*, 132(11), pp.1381–1392.

Ford, R.M. & Harvey, R.W., 2007. Role of chemotaxis in the transport of bacteria through saturated porous media. *Advances in Water Resources*, 30(6–7), pp.1608–1617.

ICOLD, 2016. *Internal erosion of existing dams, levees and dikes, and their foundations: Case histories, investigations, testing, remediation and surveillance*,

Jahns, T., 1996. Ammonium / urea-dependent generation of a proton electrochemical potential and synthesis of ATP in Bacillus pasteurii. *Journal of Bacteriology*, 178(2), pp.403–409.

Jiang, N., 2016. *Microbially Induced Calcite Precipitation for the Mitigation of Soil Internal Erosion and Sand Production*. University of Cambridge.

McNeil, J., Taylor, C. & Lick, W., 1996. Measurements of Erosion of Undisturbed Bottom Sediments with Depth. *Journal of Hydraulic Engineering-asce - J HYDRAUL ENG-ASCE*, 122.

Moody, L.F., 1944. Friction factors for pipe flow. *Trans. ASME0097-6822*, 66(671).

Mujah, D., Shahin, M.A. & Cheng, L., 2016. State-of-the-art review of bio-cementation by microbially induced calcite precipitation (MICP) for soil stabilization. *Geomicrobiology Journal*, (September), pp.00–00. Available at: https://www.tandfonline.com/doi/full/10.1080/01490451.2016.1225866.

Van Paassen, L.A., 2009. *Biogrout (ground improvement by microbially induced carbonate precipitation)*. Delft University of Technology.

Van Paassen, L.A. et al., 2010. Quantifying Biomediated Ground Improvement by Ureolysis: Large-Scale Biogrout Experiment. *Journal of Geotechnical and Geoenvironmental Engineering*, 136(12), pp.1721–1728.

Philippe, P., Beguin, R. & Faure, Y.-H., 2013. Contact Erosion. In *Erosion in Geomechanics Applied to Dams and Levees*. Hoboken, NJ, USA: John Wiley & Sons, Inc., pp. 101–191. Available at: http://doi.wiley.com/10.1002/9781118577165.ch2.

Ravens, T.M. & Gschwend, P.M., 1999. Flume measurements of sediment erodibility in Boston Harbor. *Journal of Hydraulic Engineering*, pp.998–1005.

Rebata-Landa, V., 2007. *Microbial Activity in Sediments: Effects on Soil Behavior*. Georgia Institute of Technology Atlanta, GA. Available at: http://smartech.gatech.edu/handle/1853/19720%5Cnpapers://846694d5-c111-4751-90d8-18f85506e57c/Paper/p1439.

Roberts, J., 1998. Effects of particle size and bulk density on the erosion of quartz particles. *J. Hydraul. Eng.*, 124.

Stocks-Fischer, S., Galinat, J.K. & Bang, S.S., 1999. Microbiological precipitation of CaCO3. *Soil Biology and Biochemistry*, 31(11), pp.1563–1571.

Whiffin, V.S., 2004. *Microbial CaCO3 Precipitation for the Production of Biocement*. Murdor University, Western Australia.